JACS
JOURNAL OF THE AMERICAN CHEMICAL SOCIETY
pubs.acs.org/JACS
Communication

Reinforcing Supramolecular Bonding with Magnetic Dipole Interactions to Assemble Dynamic Nanoparticle Superlattices

Peter J. Santos and Robert J. Macfarlane*

Cite This: J. Am. Chem. Soc. 2020, 142, 1170−1174
Read Online
ACCESS | Metrics & More | Article Recommendations | Supporting Information

ABSTRACT: Assembling superparamagnetic particles into ordered lattices is an attractive means of generating new magnetically responsive materials, and is commonly achieved by tailoring interparticle interactions as a function of the ligand coating. However, the inherent linkage between the collective magnetic behavior of particle arrays and the assembly processes used to generate them complicates efforts to understand and control material synthesis. Here, we use a synergistic combination of a chemical force (hydrogen bonding) and magnetic dipole coupling to assemble polymer-brush coated superparamagnetic iron oxide nanoparticles, where the relative strengths of these interactions can be tuned to reinforce one another and stabilize the resulting superlattice phases. We find that we can precisely control both the dipole−dipole coupling between nanoparticles and the strength of the ligand−ligand interactions by modifying the interparticle spacing through changes to the polymer spacer between the hydrogen bonding groups and the nanoparticles' surface. This results in modulation of the materials' blocking temperature, as well as the stabilization of a unique superlattice phase that only exists when magnetic coupling between particles is present. Using magnetic interactions to affect nanoparticle assembly in conjunction with ligand-mediated interparticle interactions expands the potential for synthesizing predictable and controllable nanoparticle-based magnetic composites.

Superparamagnetic nanoparticles can serve as building blocks for the synthesis of sophisticated materials, where hierarchical ordering of the nanoparticle constituents can modulate the collective magnetic response of the resulting structures.[1] This tunability results from magnetic dipole interactions being affected by particle composition, size, shape, and local environment. Therefore, controlling particle distribution within an assembled solid is critical for fully manipulating structure−property relationships in these magnetic materials.[2−6] A strategy for precisely dictating nanoparticle arrangement involves assembling superlattices, where the particles are driven toward the configuration that represents a thermodynamic minimum through a mixture of intermolecular interactions between the nanoparticles' ligands and the surrounding solvent.[7−9] Importantly, because magnetic dipole−dipole coupling between particles depends on the particles' positions relative to one another, these additional magnetic interactions could potentially alter the particle self-assembly pathways.[10−13] In other words, when the dipole−dipole interaction energies and ligand binding energies are balanced to be of comparable strength, the magnetic force competes with the chemical forces driving nanoparticle assembly to produce novel structures and structure−property relationships.[14−18] To achieve a self-assembly system with tailorable chemical and magnetic forces, however, a building block is needed where each interaction can be independently tuned. Magnetic coupling can be controlled by using different nanoparticle core sizes or changing interparticle spacings, while chemical interactions can be dictated by using different bonding motifs or regulating the degree of multivalency of the binding groups.[19]

We have recently described the synthesis of a nanoscale building block capable of dynamic self-assembly, the nanocomposite tecton (NCT) (Figure 1A).[20] NCTs consist of inorganic nanoparticle cores coated with polymer brushes. Each polymer chain in a brush terminates in a supramolecular binding group, and when NCTs with complementary binding groups are mixed, these bonding interactions drive NCT assembly. Previously reported NCTs have predominantly used diaminopyridine (DAP) and thymine (Thy) groups as the supramolecular binding pair, where the hydrogen bonds between DAP and Thy are thermally labile. As a result, thermal annealing enables reorganization of the assembled lattices, allowing NCTs to form crystalline architectures that maximize the number of DAP-Thy interparticle bonds.

In principle, NCTs are an ideal platform for studying the interplay between chemical bonding and magnetic coupling in nanoparticle assembly because the composition of the particle, polymer, and supramolecular binding group components of the NCT can be easily and orthogonally changed.[21] While previous NCTs used gold nanoparticle cores (AuNPs), it is also possible to use magnetically responsive nanoparticle compositions to study how magnetic interactions affect assembly. In this work, NCTs were prepared with both gold and iron oxide nanoparticle cores functionalized with polystyrene brushes that terminated in DAP and Thy groups; the AuNP NCTs served as a nonmagnetic control to isolate

Received: October 24, 2019
Published: January 6, 2020

https://dx.doi.org/10.1021/jacs.9b11476
J. Am. Chem. Soc. 2020, 142, 1170−1174

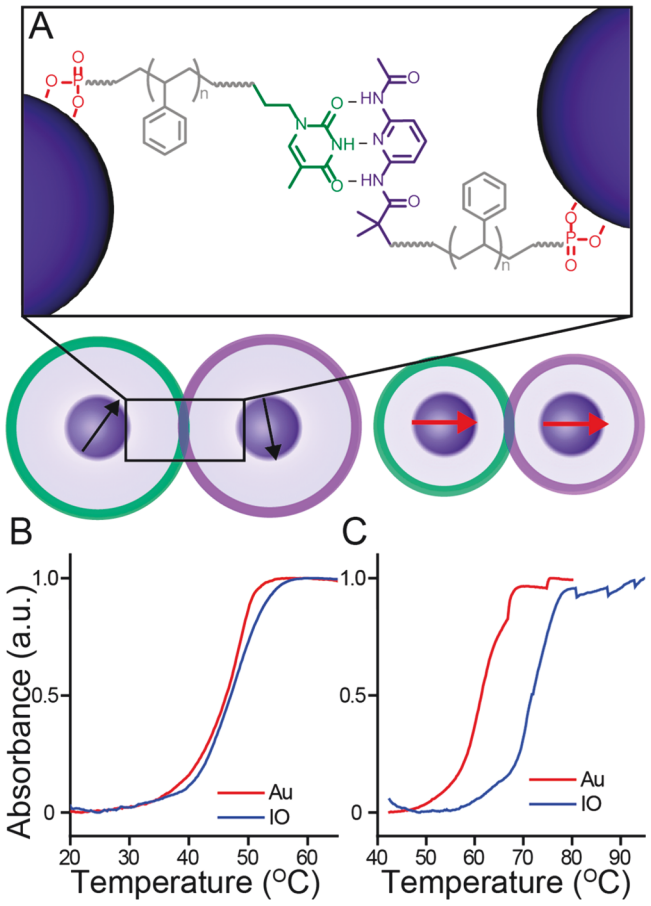

Figure 1. (A) Nanocomposite tectons (NCTs) consist of a nanoparticle core, polymer brush, and supramolecular binding groups that drive assembly. Here, iron oxide (IO) NCTs are functionalized with polystyrene chains that are modified with a terminal phosphonate anchor. Assembly is subsequently directed via complementary hydrogen bonding moieties, but can be strengthened with magnetic dipole coupling between aligned spins when interparticle distances are short. (B) Melt profiles of IO-NCTs containing 16 nm diameter IONPs with 13 kDa polymers and Au-NCTs containing 15 nm diameter AuNPs with 14 kDa polymers; the two sets of NCTs show no significant difference in their melt profiles. (C) The melting profile of 16 nm IO-NCTs coated with 8 kDa polymers is shifted ~10 °C above that of 15 nm Au-NCTs coated with 9 kDa polymers. Spikes in the data at high temperature are from evaporation and condensation of solvent.

the effects of dipole−dipole interactions on particle assembly. AuNP based NCTs were synthesized according to prior protocols.[22] The iron oxide nanoparticles (IONPs) were synthesized through the decomposition of an iron oleate precursor, resulting in 9, 14, 16, or 23 nm diameter magnetite spheres with relative standard deviations <10% (Figures S1−S3, Table S1).[23] DAP and Thy-terminated polystyrene polymers of 8 kDa and 13 kDa molecular weight with $Đ$ < 1.1 (Figure S4, Table S2) were synthesized in the same manner as reported for prior use in AuNP-based NCTs, but were instead modified with a phosphonate group at their terminus to anchor the polymers to the IONPs (further details in the Supporting Information).[24,25] TGA measurements indicate the polymers graft at a similar density to both AuNP and IONP NCTs (Figure S5), meaning that the number of DAP/Thy groups on the particles were equivalent. Isolated solutions of DAP and Thy functionalized IO-NCTs remained stable for at least a week, and did not noticeably respond when exposed to a hand-held magnet at the concentrations used in these experiments (~100 nM). After mixing DAP and Thy IO-NCTs, however, the dark solution became turbid within seconds, and aggregates became visible within a minute. The aggregates could be manipulated by a hand-held magnet, indicating their collective magnetic force could overcome Brownian motion.

Hydrogen-bonded NCTs can be cycled between assembled and melted states by changing the solution temperature; this process was monitored with UV−vis spectroscopy (Figures S6−S7).[20] For IO-NCT designs with larger interparticle spacings or smaller nanoparticle cores (e.g., 16 nm core diameter, 13 kDa polymer molecular weight), their melting temperature (T_m, the melt curve inflection point) was identical to Au-NCTs with similar design parameters (15 nm core diameter, 14 kDa polymer molecular weight) (Figure 1B). However, in systems where the ratio of particle size to interparticle distance was larger (e.g., 8 kDa polymer on 16 nm IO-NCTs, 9 kDa polymer on 15 nm Au-NCTs), T_m increased significantly (Figure 1C). We hypothesize that this added attractive energy arises from magnetic dipole coupling between particles and that these magnetic interactions are sensitive to various nanoscale structural parameters (i.e., interparticle distance and particle size; see Figure S7 for additional data).[14,16] Dipole−dipole coupling is insufficient to cause particle aggregation on its own, but can supplement the supramolecular interactions to further strengthen NCT-NCT assembly.

Because NCT assembly is governed primarily by supramolecular bonding, the two nanoparticle core compositions should be structurally equivalent when constructing nanoparticle superlattices. To confirm this, IO-NCTs and Au-NCTs were thermally annealed to drive them to their thermodynamically preferred configurations, which for complementary NCTs of identical size is a body centered cubic (bcc) lattice (Figure 2 red and blue traces).[20] This crystalline arrangement is the thermodynamic product for a range of particle sizes and polymer lengths in both the Au-NCT and IO-NCT assemblies (Figure S8).[19] Importantly, this also means that an alternating lattice of Au and IO-NCTs can be assembled if the two NCT compositions are functionalized with complementary binding groups (Figure 2, purple traces); this results in lattices structurally equivalent to CsCl crystals.[9]

Based on these structural and thermal data, we conclude that although the iron oxide cores of the NCTs are interchangeable with Au-NCTs as a structural element of the superlattices, magnetic coupling between IO-NCTs can affect the strength of interparticle bonding when IONPs are in close proximity. At larger interparticle spacings (surface to surface >5 nm), the interaction energy is best estimated by the Keesom interaction:[26]

$$U_{dd} = -\frac{1}{3k_BT}\left(\frac{m^2}{4\pi\mu_0 r^3}\right)^2 \quad (1)$$

where m is the magnetic moment (proportional to particle size), r is the interparticle distance, and μ_0 is the magnetic vacuum permeability. When assembled, each NCT is subject to interactions from neighboring particles, but because the interaction energy is approximated to change as r^{-6}, only the first few nearest neighbors would be expected to contribute to the total binding energy between neighboring NCTs.

https://dx.doi.org/10.1021/jacs.9b11476
J. Am. Chem. Soc. 2020, 142, 1170−1174

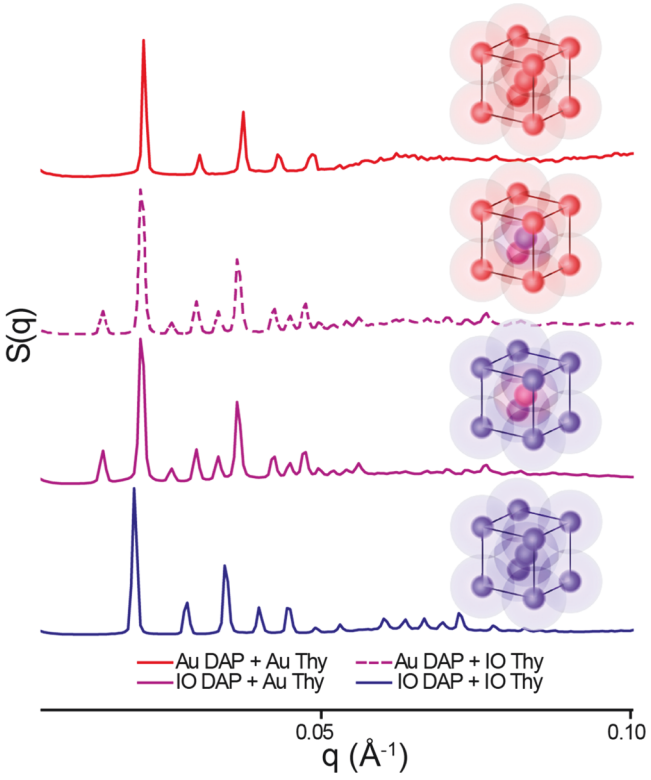

Figure 2. NCTs can be synthesized with both gold (AuNP) and iron oxide nanoparticle (IONP) cores. Small angle X-ray scattering (SAXS) patterns of superlattices assembled with IO-NCTs (bottom), Au-NCTs (top), and mixtures of Au and IO-NCTs (middle two). The lattices composed of just IONP or AuNP cores possess bcc crystal symmetry, while the combinations of IONP and AuNP have CsCl symmetry. Notably, the interparticle spacings are nearly identical, demonstrating that the superlattice crystal symmetry and lattice parameters can be independently controlled from the nanoparticle core compositions.

Furthermore, polymer ligand length should significantly affect dipole−dipole coupling strength, as it dictates the surface-to-surface distance between particles.[27] For example, 16 nm IO-NCTs functionalized with 8 kDa polymer were determined by SAXS to have a 29.6 nm interparticle spacing; eq 1 predicts that this interparticle distance should result in a dipole energy of ∼5.2 k_BT. When the polymer molecular weight is increased to 13 kDa (38.5 nm interparticle spacing), the calculated interaction energy is 1.1 k_BT. It is important to note that these magnetic dipole interaction energies are significantly weaker than a single DAP-Thy hydrogen bonding pair (12.8 k_BT in toluene),[19] but significant enough to contribute to assembly in conjunction with the supramolecular bonding.

The existence of enhanced dipole−dipole coupling for NCTs with smaller interparticle spacings can be further confirmed using zero field cooled/field cooled (ZFC/FC) measurements to determine the NCT assemblies' blocking temperatures (T_b), the temperature at which unaligned magnetic spins orient to an applied magnetic field (Figure 3, Figure S10; see Figure S11 for hysteresis measurements). Dipole−dipole interactions are known to increase T_b and broaden the temperature window of this transition.[28,29] To best determine T_b, the derivative of the difference between the ZFC and FC curves was taken for both the 8 kDa and 13 kDa linked nanoparticle assemblies mentioned above (Figure 3).[30] The peak, signifying T_b, increased by ∼11 K when the shorter

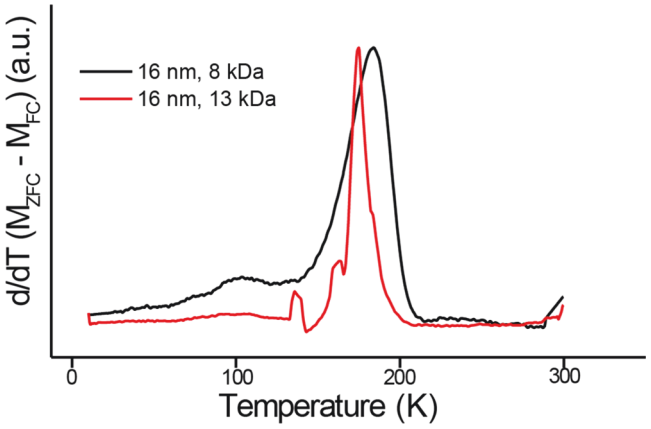

Figure 3. Blocking temperature (T_b) determination for IO-NCT assemblies with 8 kDa and 13 kDa polymer shells. T_b is identified as the peak of the derivative of the difference between the zero field cooled (ZFC) and field cooled (FC) curves (see Figure S10 for experimental data). Upon shortening the polymer length, the T_b increases and the transition range broadens, indicating an increase in dipole−dipole interactions.

polymer was used, and the transition significantly broadened, confirming an enhancement in dipole−dipole interactions.

The observed increases in T_m and T_b are consistent with the notion that shortening the interparticle distance between IO-NCTs allows the magnetic polarization of each particle to interact and increase the interparticle attraction. Adding magnetic coupling therefore contributes another design parameter for controlling nanoparticle assembly, and consequently it may be possible to stabilize particle systems that otherwise may not crystallize. Indeed, IO-NCTs synthesized with the shorter Thy-terminated polymer ligand formed face centered cubic (fcc) lattices when prepared in the absence of DAP-NCTs, the first time this phase has been demonstrated in the NCT system. While Thy-Thy interactions can be stabilized by hydrogen bonding,[31] these interactions are too weak on their own to cause the Thy-coated NCTs to assemble into stable lattices. Accordingly, Au-NCTs functionalized with short Thy polymers (9 kDa) exhibit only a slight scattering peak (Figure 4, red data). However, the well-defined fcc crystals formed by IO-NCTs imply that an additional magnetic attractive force must be present (Figure 4, blue data).[32] Consistent with this observation, no assembly occurs between IO-NCTs functionalized with longer Thy-terminated polymers (Figure S9).

We have demonstrated that the NCT design concept is easily adapted to magnetic nanoparticles, making NCTs a powerful platform for designing magnetic nanocomposites. NCTs can be appropriately designed to either mask the identity of the core composition or take advantage of any inherent interparticle interactions, with some limitations based on nanoparticle size and interparticle spacings. Due to the complex sets of interactions governing self-assembly in these magnetic NCTs, magnetic dipole coupling between nanoparticles can reinforce the supramolecular interactions that drive the formation of superlattices. These synergistic interactions can even stabilize previously unachievable crystallographic symmetries. Consequently, NCTs can further clarify the interactions of nanoscale materials and how the competition between forces affects self-assembly. Furthermore, the ability to engineer the magnetic coupling of nanoparticles

https://dx.doi.org/10.1021/jacs.9b11476
J. Am. Chem. Soc. 2020, 142, 1170−1174

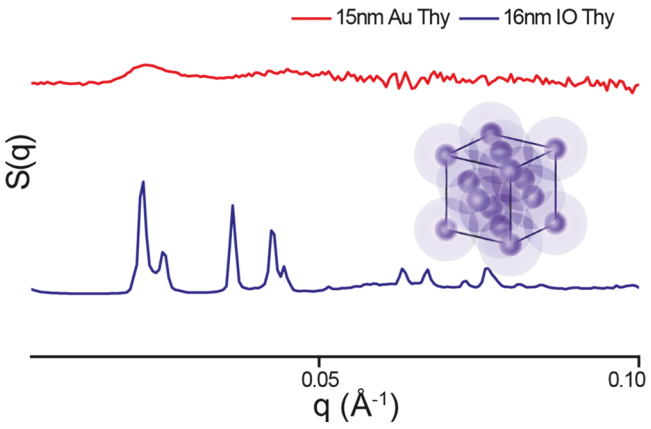

Figure 4. 15 nm Au-NCTs functionalized with ∼9 kDa Thy-terminated polymers exhibit a slight peak at q = 0.023 Å^{-1} indicating only minor amounts of random aggregation. Conversely, 16 nm IO-NCTs functionalized with ∼8 kDa Thy-terminated polymers show the sharp and clear scatting pattern of a face centered cubic (fcc) superlattice.

is a promising strategy to developing materials with complex metamaterial properties.

■ ASSOCIATED CONTENT

Supporting Information

The Supporting Information is available free of charge at https://pubs.acs.org/doi/10.1021/jacs.9b11476.

Materials and Methods; Scheme S1; Figures S1−S9; Tables S1−S3; Supplementary References 1−7 (PDF)

■ AUTHOR INFORMATION

Corresponding Author

Robert J. Macfarlane − *Massachusetts Institute of Technology, Cambridge, Massachusetts;* orcid.org/0000-0001-9449-2680; Email: rmacfarl@mit.edu

Other Author

Peter J. Santos − *Massachusetts Institute of Technology, Cambridge, Massachusetts*

Complete contact information is available at: https://pubs.acs.org/10.1021/jacs.9b11476

Notes

The authors declare no competing financial interest.

■ ACKNOWLEDGMENTS

This work was primarily supported by an NSF CAREER grant, Award Number CHE-1653289, supported in part by the U.S. Army Research Office under Grant W911NF-18-1-0197, and made use of the MRSEC Shared Experimental Facilities at MIT, supported by the NSF under Award DMR 14-19807. P.J.S. acknowledges support by the NSF Graduate Research Fellowship Program under Grant 1122374. SAXS experiments at beamline 12-ID-B at the Advanced Photon Source at Argonne National Laboratory were supported by the U.S. Department of Energy, Office of Science, Office of Basic Energy Sciences, under Contract DE-AC02-06CH11357.

■ REFERENCES

(1) Majetich, S. A.; Wen, T.; Booth, R. A. Functional Magnetic Nanoparticle Assemblies: Formation, Collective Behavior, and Future Directions. *ACS Nano* **2011**, *5* (8), 6081−6084.

(2) Feld, A.; Koll, R.; Fruhner, L. S.; Krutyeva, M.; Pyckhout-Hintzen, W.; Weiß, C.; Heller, H.; Weimer, A.; Schmidtke, C.; Appavou, M.-S.; Kentzinger, E.; Allgaier, J.; Weller, H. Nanocomposites of Highly Monodisperse Encapsulated Superparamagnetic Iron Oxide Nanocrystals Homogeneously Dispersed in a Poly(Ethylene Oxide) Melt. *ACS Nano* **2017**, *11* (4), 3767−3775.

(3) Cheon, J.; Park, J.-I.; Choi, J.; Jun, Y.; Kim, S.; Kim, M. G.; Kim, Y.-M.; Kim, Y. J. Magnetic Superlattices and Their Nanoscale Phase Transition Effects. *Proc. Natl. Acad. Sci. U. S. A.* **2006**, *103* (9), 3023−3027.

(4) Yang, Z.; Wei, J.; Bonville, P.; Pileni, M.-P. Engineering the Magnetic Dipolar Interactions in 3D Binary Supracrystals Via Mesoscale Alloying. *Adv. Funct. Mater.* **2015**, *25* (30), 4908−4915.

(5) Jishkariani, D.; Lee, J. D.; Yun, H.; Paik, T.; Kikkawa, J. M.; Kagan, C. R.; Donnio, B.; Murray, C. B. The Dendritic Effect and Magnetic Permeability in Dendron Coated Nickel and Manganese Zinc Ferrite Nanoparticles. *Nanoscale* **2017**, *9* (37), 13922−13928.

(6) Yeom, J.; Santos, U. S.; Chekini, M.; Cha, M.; de Moura, A. F.; Kotov, N. A. Chiromagnetic Nanoparticles and Gels. *Science* **2018**, *359* (6373), 309−314.

(7) Shevchenko, E. V.; Talapin, D. V.; Kotov, N. A.; O'Brien, S.; Murray, C. B. Structural Diversity in Binary Nanoparticle Superlattices. *Nature* **2006**, *439* (7072), 55−59.

(8) Nayak, S.; Horst, N.; Zhang, H.; Wang, W.; Mallapragada, S.; Travesset, A.; Vaknin, D. Interpolymer Complexation as a Strategy for Nanoparticle Assembly and Crystallization. *J. Phys. Chem. C* **2019**, *123* (1), 836−840.

(9) Zhang, C.; Macfarlane, R. J.; Young, K. L.; Choi, C. H. J.; Hao, L.; Auyeung, E.; Liu, G.; Zhou, X.; Mirkin, C. A. A General Approach to DNA-Programmable Atom Equivalents. *Nat. Mater.* **2013**, *12* (8), 741−746.

(10) Singh, G.; Chan, H.; Baskin, A.; Gelman, E.; Repnin, N.; Král, P.; Klajn, R. Self-Assembly of Magnetite Nanocubes into Helical Superstructures. *Science* **2014**, *345* (6201), 1149−1153.

(11) Nonappa; Haataja, J. S.; Timonen, J. V. I.; Malola, S.; Engelhardt, P.; Houbenov, N.; Lahtinen, M.; Häkkinen, H.; Ikkala, O. Reversible Supracolloidal Self-Assembly of Cobalt Nanoparticles to Hollow Capsids and Their Superstructures. *Angew. Chem., Int. Ed.* **2017**, *56* (23), 6473−6477.

(12) Ahniyaz, A.; Sakamoto, Y.; Bergström, L. Magnetic Field-Induced Assembly of Oriented Superlattices from Maghemite Nanocubes. *Proc. Natl. Acad. Sci. U. S. A.* **2007**, *104* (45), 17570−17574.

(13) Yang, Y.; Wang, B.; Shen, X.; Yao, L.; Wang, L.; Chen, X.; Xie, S.; Li, T.; Hu, J.; Yang, D.; Dong, A. Scalable Assembly of Crystalline Binary Nanocrystal Superparticles and Their Enhanced Magnetic and Electrochemical Properties. *J. Am. Chem. Soc.* **2018**, *140* (44), 15038−15047.

(14) Talapin, D. V.; Shevchenko, E. V.; Murray, C. B.; Titov, A. V.; Král, P. Dipole−Dipole Interactions in Nanoparticle Superlattices. *Nano Lett.* **2007**, *7* (5), 1213−1219.

(15) Lalatonne, Y.; Richardi, J.; Pileni, M. P. Van Der Waals versus Dipolar Forces Controlling Mesoscopic Organizations of Magnetic Nanocrystals. *Nat. Mater.* **2004**, *3* (2), 121.

(16) Chen, J.; Dong, A.; Cai, J.; Ye, X.; Kang, Y.; Kikkawa, J. M.; Murray, C. B. Collective Dipolar Interactions in Self-Assembled Magnetic Binary Nanocrystal Superlattice Membranes. *Nano Lett.* **2010**, *10* (12), 5103−5108.

(17) Frankamp, B. L.; Boal, A. K.; Tuominen, M. T.; Rotello, V. M. Direct Control of the Magnetic Interaction between Iron Oxide Nanoparticles through Dendrimer-Mediated Self-Assembly. *J. Am. Chem. Soc.* **2005**, *127* (27), 9731−9735.

(18) Yang, Z.; Wei, J.; Bonville, P.; Pileni, M.-P. Beyond Entropy: Magnetic Forces Induce Formation of Quasicrystalline Structure in

Binary Nanocrystal Superlattices. *J. Am. Chem. Soc.* **2015**, *137* (13), 4487−4493.
(19) Santos, P. J.; Cao, Z.; Zhang, J.; Alexander-Katz, A.; Macfarlane, R. J. Dictating Nanoparticle Assembly via Systems-Level Control of Molecular Multivalency. *J. Am. Chem. Soc.* **2019**, *141* (37), 14624−14632.
(20) Zhang, J.; Santos, P. J.; Gabrys, P. A.; Lee, S.; Liu, C.; Macfarlane, R. J. Self-Assembling Nanocomposite Tectons. *J. Am. Chem. Soc.* **2016**, *138* (50), 16228−16231.
(21) Wang, Y.; Santos, P. J.; Kubiak, J. M.; Guo, X.; Lee, M. S.; Macfarlane, R. J. Multistimuli Responsive Nanocomposite Tectons for Pathway Dependent Self-Assembly and Acceleration of Covalent Bond Formation. *J. Am. Chem. Soc.* **2019**, *141* (33), 13234−13243.
(22) Santos, P. J.; Cheung, T. C.; Macfarlane, R. J. Assembling Ordered Crystals with Disperse Building Blocks. *Nano Lett.* **2019**, *19* (8), 5774−5780.
(23) Noh, H.-J.; Park, J.-H.; Kim, J.-Y.; Park, J.-G.; Park, J.; An, K.; Hwang, N.-M.; Hyeon, T.; Hwang, Y. Ultra-Large-Scale Syntheses of Monodisperse Nanocrystals. *Nat. Mater.* **2004**, *3* (12), 891.
(24) Matyjaszewski, K.; Xia, J. Atom Transfer Radical Polymerization. *Chem. Rev.* **2001**, *101* (9), 2921−2990.
(25) Turcheniuk, K.; Tarasevych, A. V.; Kukhar, V. P.; Boukherroub, R.; Szunerits, S. Recent Advances in Surface Chemistry Strategies for the Fabrication of Functional Iron Oxide Based Magnetic Nanoparticles. *Nanoscale* **2013**, *5* (22), 10729−10752.
(26) Bishop, K. J. M.; Wilmer, C. E.; Soh, S.; Grzybowski, B. A. Nanoscale Forces and Their Uses in Self-Assembly. *Small* **2009**, *5* (14), 1600−1630.
(27) Boal, A. K.; Frankamp, B. L.; Uzun, O.; Tuominen, M. T.; Rotello, V. M. Modulation of Spacing and Magnetic Properties of Iron Oxide Nanoparticles through Polymer-Mediated "Bricks and Mortar" Self-Assembly. *Chem. Mater.* **2004**, *16* (17), 3252−3256.
(28) Majetich, S. A.; Sachan, M. Magnetostatic Interactions in Magnetic Nanoparticle Assemblies: Energy, Time and Length Scales. *J. Phys. D: Appl. Phys.* **2006**, *39* (21), R407−R422.
(29) Hou, Y.; Yu, J.; Gao, S. Solvothermal Reduction Synthesis and Characterization of Superparamagnetic Magnetite Nanoparticles. *J. Mater. Chem.* **2003**, *13* (8), 1983−1987.
(30) Bruvera, I. J.; Mendoza Zélis, P.; Pilar Calatayud, M.; Goya, G. F.; Sánchez, F. H. Determination of the Blocking Temperature of Magnetic Nanoparticles: The Good, the Bad, and the Ugly. *J. Appl. Phys.* **2015**, *118* (18), 184304.
(31) Dey, M.; Moritz, F.; Grotemeyer, J.; Schlag, E. W. Base Pair Formation of Free Nucleobases and Mononucleosides in the Gas Phase. *J. Am. Chem. Soc.* **1994**, *116* (20), 9211−9215.
(32) Macfarlane, R. J.; Lee, B.; Jones, M. R.; Harris, N.; Schatz, G. C.; Mirkin, C. A. Nanoparticle Superlattice Engineering with DNA. *Science* **2011**, *334* (6053), 204−208.

https://dx.doi.org/10.1021/jacs.9b11476
J. Am. Chem. Soc. 2020, 142, 1170−1174